

Intelligence computing approach for solving second order system of Emden–Fowler model

Zulqurnain Sabir^{1, *}, Fazli Amin^{1, a}, Daniel Pohl², Juan L.G. Guirao⁴

¹Department of Mathematics and Statistics, Hazara University, Mansehra, Pakistan

*Email: zulqurnain_maths@hu.edu.pk

^aEmail: fazliamin@hu.edu.pk

²Design Engineering, Kinectrics Inc., Toronto, Ontario, Canada

Email: daniel.Pohl@Kinectrics.com

⁴Department of Applied Mathematics and Statistics, Technical University of Cartagena, Hospital de Marina 30203-Cartagena, Spain

Email: juan.garcia@upct.es

Abstract: In this research study, an advance computational intelligence paradigm is used for solving second order Emden-Fowler system (EFS) based on artificial neural network, genetic algorithm (GA) which is famous global search method, sequential quadratic programming (SQP) known as rapid local refinement and the hybrid of GA-SQP. The proficiency of the designed scheme is inspected by solving the three examples of EFS to check the efficiency, consistency, precision and exactness of the technique. The numerical outcomes of the purposed scheme are compared with the exact solution that shows the significance of the scheme based on accuracy, correctness and convergence. Moreover, statistical explorations have been executed to verify the precision and accuracy of the outcomes based on performance measures of mean absolute deviation, root mean squared error and variance account for.

Keywords: Emden-Fowler system, artificial neural network, genetic algorithm, sequential quadratic programming, statistical analysis.

1. Introduction

The Lane-Emden model (LEM) is the fundamental model introduced by Lane and further explored by Emden has many applications and widely use to study the stellar structure. This model has a great history and broad applications in the density profile of gaseous star [1], mathematical physics and geometry [2], catalytic diffusion reactions [3], polytropic and isothermal gas spheres [4], electromagnetic theory [5], oscillating magnetic fields [6], classical and quantum mechanics [7], isotropic continuous media [8], dusty fluid models [9] and morphogenesis [10]. Many techniques have been implemented to solve this challenging and famous singular LEM. To mention the few of them, Bender et al [11] applied perturbative method, Shawagfeh [12] proposed Adomian decomposition method, Liao [13] suggested an analysis algorithm, Nouh [14] applied power series by using an Euler-Abel and Pade approximation, Mandelzweigand and Tabakin [15] developed Bellman and Kalabas quasi linearization method for solving these type of singular problems. The Emden–Fowler system (EFS) is used to model the several phenomena, like as population evolution, pattern formation and chemical reactions. The general form of EFS can be expressed as [16, 17]

$$\begin{cases} u'' + \frac{\mu_1}{t} u' + g(u, v) = f(t), & u(0) = a_1, u'(0) = 0, \\ v'' + \frac{\mu_2}{t} v' + g(u, v) = s(t), & v(0) = a_2, v'(0) = 0. \end{cases} \quad (1)$$

Where μ_1 and μ_2 are positive constants. All the above-mentioned techniques have their own performance, accuracy and efficiency, as well as imperfections over one another. The heuristic techniques based on the stochastic type of solvers optimize with linear/nonlinear models by manipulating the neural network's strength and practical adaptation of the applications of evolutionary computing [18-19]. Some possible recent applications are Thomas-Fermi atom's model [20], uncertainties in computational mechanics [21], nonlinear singular functional differential model [22], transistor-level uncertainty quantification [23], heartbeat model [24], control systems [25], cell biology [26], power [27] and energy [28].

The intention of the recent study is to present numerical solutions of EFS (1) using intelligent computing technique based on the strength of artificial neural networks (ANNs) optimized with genetic algorithm (GA) supported by sequential quadratic programming (SQP). The salient features of the scheme are summarized as:

- ANNs applied successfully and effectively for solving the three variants of nonlinear singular system of Emden-Fowler equations.
- Investigation and manipulation via neural networks based stochastic solvers are applied to find the accurate and consistent numerical outcomes for the nonlinear EFS.
- The consistent overlapping with the present outcomes and the exact solutions established the stability and correctness of the designed scheme.
- The performance measures through statistics based operators is checked using 100 independent runs give more satisfaction of the designed scheme
- EFS is not easy to solve due to the nonlinear behavior and singularity. ANN is a good selection to handle such kind of complicated problems where the other conventional/traditional techniques fail.

2. Design Methodology

For the solution of Emden-Fowler system (EFS), the designed proposed methodology based on two phases: first phase is to use an error based fitness function based on the differential equation of the EFS. While the second phase is to provide the detailed discussions using the hybrid of GA-SQP.

2.1 Modeling

The mathematical description of the EFS (1) is formulated to feed-forward ANNs in the form of $u(t)$ and $v(t)$, as well as, their respective n th order derivatives are given as:

$$[\hat{u}(t), \hat{v}(t)] = \left[\sum_{j=1}^m \varphi_{h,j} h(w_{u,j} t + b_{u,j}), \sum_{j=1}^m \varphi_{f,j} h(w_{v,j} t + b_{v,j}) \right], \quad (2)$$

$$[\hat{u}^{(n)}, \hat{v}^{(n)}] = \left[\sum_{j=1}^m \varphi_{u,j} h^{(n)}(w_{u,j}t + b_{u,j}), \sum_{j=1}^m \varphi_{v,j} h^{(n)}(w_{v,j}t + b_{v,j}) \right]$$

Where the number of neurons are denoted by m , while the n represents derivative order. The terms φ , w and b are the unknown weight vector \mathbf{W} defined as:

$\mathbf{W} = [\mathbf{W}_u, \mathbf{W}_v]$, for $\mathbf{W}_u = [\varphi_u, \mathbf{w}_u, \mathbf{b}_u]$ and $\mathbf{W}_v = [\varphi_v, \mathbf{w}_v, \mathbf{b}_v]$. The components of weight vector are given as:

$$\begin{aligned} \varphi_u &= [\varphi_{u,1}, \varphi_{u,2}, \dots, \varphi_{u,m}], & \varphi_v &= [\varphi_{v,1}, \varphi_{v,2}, \dots, \varphi_{v,m}], \\ \mathbf{w}_u &= [w_{u,1}, w_{u,2}, \dots, w_{u,m}], & \mathbf{w}_v &= [w_{v,1}, w_{v,2}, \dots, w_{v,m}], \\ \mathbf{b}_u &= [b_{u,1}, b_{u,2}, \dots, b_{u,m}], & \mathbf{b}_v &= [b_{v,1}, b_{v,2}, \dots, b_{v,m}]. \end{aligned}$$

Using $h(t) = 1/(1+e^{-t})$ i.e., log-sigmoid activation function, the network (2) is updated using the approximate values of $\hat{u}(t)$ and $\hat{v}(t)$ with their first and second order derivatives are respectively given as:

$$\begin{aligned} [\hat{u}(t), \hat{v}(t)] &= \left[\sum_{j=1}^m \frac{\varphi_{u,j}}{1 + e^{-(w_{u,j}t + b_{u,j})}}, \sum_{j=1}^m \frac{\varphi_{v,j}}{1 + e^{-(w_{v,j}t + b_{v,j})}} \right], \\ [\hat{u}'(t), \hat{v}'(t)] &= \left[\sum_{j=1}^m \frac{\varphi_{u,j} w_{u,j} e^{-(w_{u,j}t + b_{u,j})}}{\left(1 + e^{-(w_{u,j}t + b_{u,j})}\right)^2}, \sum_{j=1}^m \frac{\varphi_{v,j} w_{v,j} e^{-(w_{v,j}t + b_{v,j})}}{\left(1 + e^{-(w_{v,j}t + b_{v,j})}\right)^2} \right], \\ [\hat{u}''(t), \hat{v}''(t)] &= \left[\sum_{j=1}^m \varphi_{u,j} w_{u,j}^2 \left\{ \frac{2e^{-2(w_{u,j}t + b_{u,j})}}{\left(1 + e^{-(w_{u,j}t + b_{u,j})}\right)^3} - \frac{e^{-(w_{u,j}t + b_{u,j})}}{\left(1 + e^{-(w_{u,j}t + b_{u,j})}\right)^2} \right\}, \right. \\ &\quad \left. \sum_{j=1}^m \varphi_{v,j} w_{v,j}^2 \left\{ \frac{2e^{-2(w_{v,j}t + b_{v,j})}}{\left(1 + e^{-(w_{v,j}t + b_{v,j})}\right)^3} - \frac{e^{-(w_{v,j}t + b_{v,j})}}{\left(1 + e^{-(w_{v,j}t + b_{v,j})}\right)^2} \right\} \right] \end{aligned} \quad (3)$$

Using the network (3), the fitness function in the sense of mean squared error is written as:

$$\epsilon = \epsilon_1 + \epsilon_2 + \epsilon_3 \quad (4)$$

$$\epsilon_1 = \frac{1}{N} \sum_{m=1}^N (t^* u_m'' + \mu_1 u' + t^* g(u_m, v_n) - t^* f_m)^2, \quad (5)$$

$$\epsilon_2 = \frac{1}{N} \sum_{m=1}^N (t^* v_m'' + \mu_2 v' + t^* g(u_m, v_n) - t^* s_m)^2, \quad (6)$$

$$N = \frac{1}{h}, \quad \hat{u}_m = \hat{u}(t_m), \quad \hat{v}_m = \hat{v}(t_m), \quad t_m = mh,$$

Where, ϵ_1 and ϵ_2 are error functions related to the EMS, the approximate solutions are denoted as $[\hat{u}(t), \hat{v}(t)]$. Whereas, the error function ϵ_3 related to initial conditions, given as:

$$\epsilon_3 = \frac{1}{2} \left((\hat{u}_0 - a_1)^2 + (\hat{v}_0 - a_2)^2 \right) \quad (7)$$

The solution of the EFS (1) can be achieved to the available appropriate weights, the fitness function ϵ tends to zero, *i.e.*, $\epsilon \rightarrow 0$, then, the approximate solutions *i.e.*, $[\hat{u}(t), \hat{v}(t)]$ identical with the desired results, *i.e.*, $[\hat{u}(t) \rightarrow u(t)]$ and $[\hat{v}(t) \rightarrow v(t)]$.

2.2 Optimization of networks

A vital explanation of the optimization to get the design parameter values of ANNs on the basis of GAs combined with SQP given as:

Genetic Algorithm: population of candidate solution in genetic algorithm known as creatures or phenotypes, individuals to an optimization problem, which is progressing toward improved solutions. Each applicant solution has a property set (chromosomes) that can be transformed or improved. Usually, results are signified in binary form as strings of zeros and ones. The evolution normally starts from a population of randomly made individuals, which is an iterative process and it became generation with the population. The fitness values of each individual in the population are calculated on each iteration. GA has a variety of applications in many fields of technologies, engineering and applied sciences. Recently, GAs used to optimize heterogeneous bin packing [29], emergency humanitarian logistics scheduling [30], cost optimized for a multi-energy source building [31], traveling salesman problem [32], the optimal set of overlapping clusters [33], design of buildings for residential buildings [34], new encoding on the basis of least spanning tree for the reconfiguration of feeder distribution [35], wind power system [36], an implementation of intrusion detection system [37], determination of glass transitions in boiling candies [38] and in the design of military surveillance networks [39]. The GA becomes faster through the hybridization procedure with the appropriate local search method.

Sequential Quadratic Programming: It is implemented for solving the optimization sub-problems sequence. In this regards, an objective function is optimized due to linearization of the constraints. For unconstrained problem, the method diminishes to Newton method for finding a point, where the gradient of the objective vanishes. For equality constraints, the method is equivalent to apply the Newton's method to the first-order optimality conditions, or Karush–Kuhn–Tucker conditions, of the problem. Some recent application of SQP is multiproduct economic production [40], economic load dispatch problem [41], optimal attitude and flight vector recovery for large transport aircraft [42], bipedal dynamic walking robot [43] and short-term hydrothermal coordination.

In this study, the hybrid strength of GA-SQP is oppressed for design variability of the networks to solve the EFS. GA-SQP steps in the workflow diagram are provided in Fig. 1, whereas the detail of GA-SQP pseudocode is given in Table 1.

2.3 Performance Metrics

The performance measures based on the mean absolute deviation (MAD), root mean squared error (RMSE), and variance account for (VAF) are investigated on the functioning of the designed method. Mathematical form for both $u(t)$ and $v(t)$ of EFS in the form of MAD, RMSE and VAF are given, respectively, as:

$$[MAD_u, MAD_v] = \left[\frac{1}{m} \sum_{j=1}^m |u(t_j) - \hat{u}(t_j)|, \frac{1}{m} \sum_{j=1}^m |v(t_j) - \hat{v}(t_j)| \right], \quad (8)$$

$$[RMSE_u, RMSE_v] = \left[\sqrt{\frac{1}{m} \sum_{j=1}^m (u(t_j) - \hat{u}(t_j))^2}, \sqrt{\frac{1}{m} \sum_{j=1}^m (v(t_j) - \hat{v}(t_j))^2} \right], \quad (9)$$

$$[VAF_u, VAF_v] = \left[\left(1 - \frac{\text{var}\{u(t_j) - \hat{u}(t_j)\}}{\text{var } u(t_j)} \right) * 100, \left(1 - \frac{\text{var}\{v(t_j) - \hat{v}(t_j)\}}{\text{var } v(t_j)} \right) * 100 \right]. \quad (10)$$

The error function $EVAF$ related to VAF mathematically given as:

$$[EVAF_u, EVAF_v] = [100 - VAF_u, 100 - VAF_v] \quad (11)$$

Where, m represents the grid points. Global description of MAD, RMSE and VAF are formulated on the mean values of these operators over numerous independent runs. Mathematically, global variations of performance indices are indicated as, Global MAD (GMAD), Global RMSD (GRMSD) and Global VAF (GVAF) are used to scrutinize the designed methodology for solving the EFS.

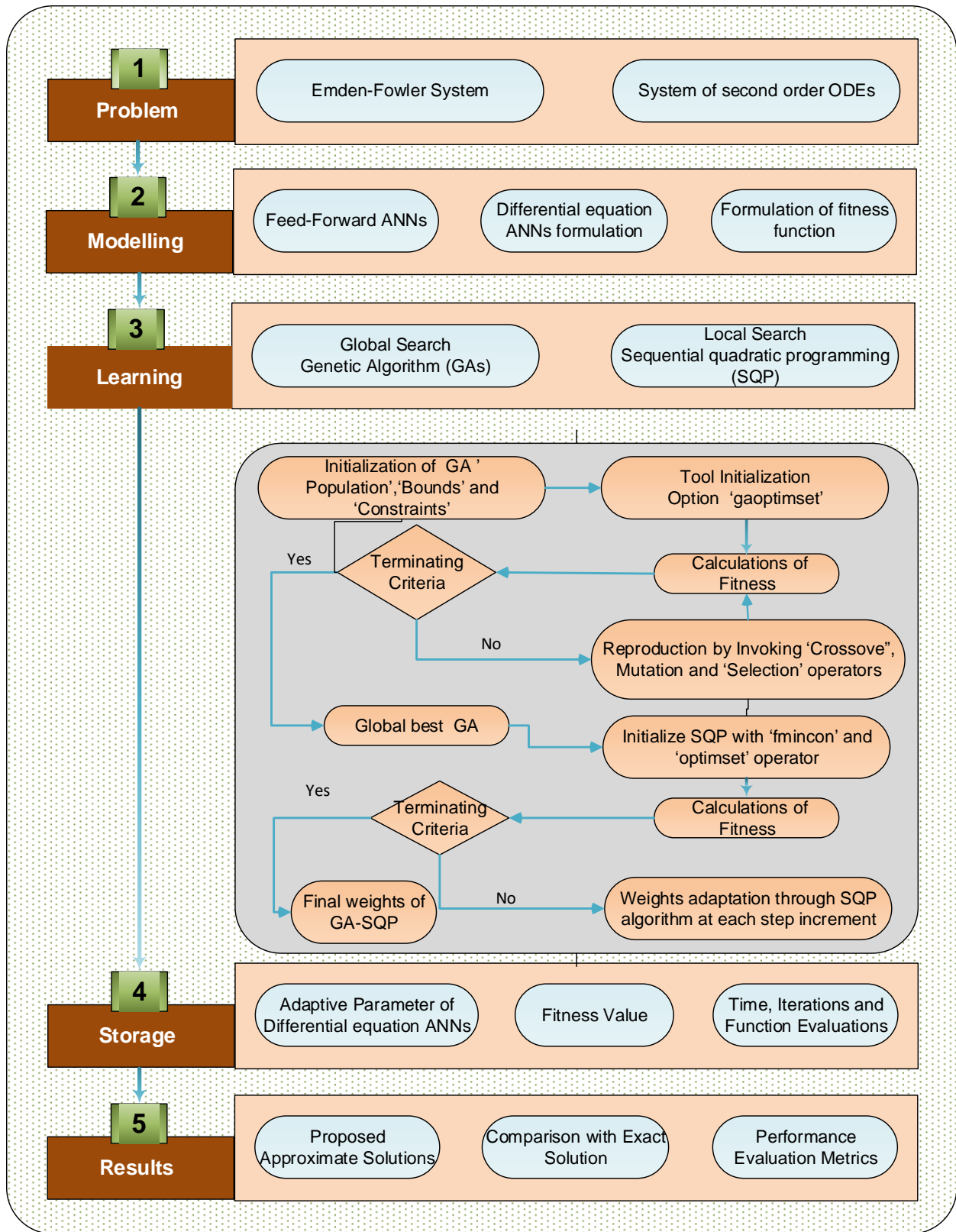


Fig 1. Workflow diagram of the proposed methodology

Table 1: Pseudo code for GA-SQP to optimize the systems

Start of Genetic Algorithms

Inputs:

The chromosome signified with same number of entries of Networks as:

$$W = [W_u, W_v] = [(\varphi_u, w_u, b_u), (\varphi_v, w_v, b_v)]$$

$$\varphi_u = [\varphi_{u,1}, \varphi_{u,2}, \dots, \varphi_{u,m}], \varphi_v = [\varphi_{v,1}, \varphi_{v,2}, \dots, \varphi_{v,m}], w_u = [w_{u,1}, w_{u,2}, \dots, w_{u,m}],$$

$$w_v = [w_{v,1}, w_{v,2}, \dots, w_{v,m}], b_u = [b_{u,1}, b_{u,2}, \dots, b_{u,m}], b_v = [b_{v,1}, b_{v,2}, \dots, b_{v,m}].$$

Population: chromosome's set is indicated as:

$$P = [(W_{u1}, W_{u2}, W_{u3}, \dots, W_{un}), (W_{v1}, W_{v2}, W_{v2}, \dots, W_{vn})]$$

$$[W_{uj}, W_{vj}] = [(\varphi_{uj}, w_{uj}, b_{uj}), (\varphi_{vj}, w_{vj}, b_{vj})]$$

Output: Global best individual of GAs is denoted as $W_{GA-Best}$

Initialization

Produce a W vector of real confined numbers to denote a chromosome. To form an initial P Set of W used. Set Generation and declarations values of "GA" and "gaoptimset" procedures

Calculations of Fitness

Achieved the fitness ϵ using equation (4) for all W in P

Termination

Implementation of the scheme terminates for accomplishment of the following

'Fitness limit = $e \rightarrow 10^{-12}$ ', 'Generations = 100', 'TolFun $\rightarrow 10^{-18}$,
'TolCon $\rightarrow 10^{-20}$, 'StallGenLimit $\rightarrow 75$, 'PopulationSize $\rightarrow 200$ ' and other values are taken as default

Go to **storage** step, If termination condition meets,

Ranking

Each W of P ranked through excellence of the fitness rate.

Reproduction

Repeated the new P with following hands at each iteration

- 'Selection': "@selectionuniform".
- 'Crossover': "@crossoverheuristic routine".
- 'Mutations': "@mutationadaptfeasible function".
- 'Elitism': "best ranked chromosome of P ".

Continue from **fitness** step

Storage

$W_{GA-Best}$ store, fitness, time, generation and count of functions for the current run of GAs

End Genetic algorithms

GA-SQP Procedure Start

Inputs

Best global vector $W_{GA-Best}$

Output

GA-SQP is the best weight vector, i.e., W_{GA-SQP}

Initialize

Use start point $W_{GA-Best}$

Decelerations and bounded are prepared for the 'optimset' and 'fmincon' routines,

Termination

Algorithm stop, any of the value meet
'Fitness limit = $e \leq 10^{-14}$, 'total Iterations = 800', 'TolFun $\leq 10^{-18}$, 'TolX $\leq 10^{-18}$, 'TolCon $\leq 10^{-20}$, or MaxFunEvals ≤ 200000

While (Terminate)
Fitness calculation
Using equations (4-7), find the fitness ϵ of present weight vector
Adjustments
Invoking "fmincon" routine using algorithm "SQP" to adjust weight vector for each incremental phase in iteration.
Go to the step of fitness with update weight vector \mathbf{W}

End
Save the final adaptive weights \mathbf{W}_{GA-SQP} and its fitness, iterations, time and function assessed for the current run.

GA-SQP Procedure End

Statistics

Repeat the GA-SQP procedure for 100 times to train the networks for the outcomes of EFS and collected data is used for effective Statistics

3. Simulations and results

The numerical study of the proposed methodology is narrated to investigate the EFS. Comparison of results are made with the exact solutions for three examples

Example 1: Consider the nonlinear EFS is

$$\begin{cases} u'' + \frac{1}{t}u' + u^2v - (4t^2 + 5)u = 0, & u(0) = 1, u'(0) = 0, \\ v'' + \frac{2}{t}v' + uv^2 - (4t^2 - 5)v = 0, & v(0) = 1, v'(0) = 0. \end{cases} \quad (12)$$

The fitness function of the system (12) is

$$\epsilon = \frac{1}{N} \sum_{m=0}^N \left(\left(t_m \hat{u}_m'' + \hat{u}_m' + t_m \hat{u}_m^2 \hat{v}_m - (4t_m^3 + 5t_m) \hat{u}_m \right)^2 + \left(t_m \hat{v}_m'' + 2\hat{v}_m' + t_m \hat{u}_m \hat{v}_m^2 - (4t_m^3 - 5t_m) \hat{v}_m \right)^2 \right) + \frac{1}{4} \left((\hat{u}_0 - 1)^2 + (\hat{v}_0 - 1)^2 + (\hat{u}_0')^2 + (\hat{v}_0')^2 \right) \quad (13)$$

Example 2: Consider the nonlinear EFS is

$$\begin{cases} u'' + \frac{2}{t}u' + v^2 - u^2 + 6v = 6t^2 + 6, & u(0) = 1, u'(0) = 0, \\ v'' + \frac{2}{t}v' + u^2 - v^2 - 6v = -6t^2 + 6, & v(0) = 1, v'(0) = 0. \end{cases} \quad (14)$$

The formulation of the fitness function is

$$\epsilon = \frac{1}{N} \sum_{m=0}^N \left(\left(t_m \hat{u}_m'' + 2\hat{u}_m' + t_m \hat{v}_m^2 - t_m \hat{u}_m^2 + 6t_m \hat{v}_m - 6t_m^3 - 6t_m \right)^2 + \left(t_m \hat{v}_m'' + 2\hat{v}_m' + t_m \hat{u}_m^2 - t_m \hat{v}_m^2 - 6t_m \hat{v}_m + 6t_m^3 - 6t_m \right)^2 \right) + \frac{1}{4} \left((\hat{u}_0 - 1)^2 + (\hat{v}_0 - 1)^2 + (\hat{u}_0')^2 + (\hat{v}_0')^2 \right) \quad (15)$$

Example 3: Consider the EFS having strong nonlinearity

$$\begin{cases} u'' + \frac{3}{t}u' + uv + (t^2 + 4)u^5 = 1, & u(0) = 1, u'(0) = 0, \\ v'' + \frac{4}{t}v' + uv - (4t^2 + 5)u^3 = 1, & v(0) = 1, v'(0) = 0. \end{cases} \quad (16)$$

The fitness function of the model (16) is

$$\epsilon = \frac{1}{N} \sum_{m=0}^N \left(\left(t_m \hat{u}_m'' + 3\hat{u}_m' + t_m \hat{u}_m \hat{v}_m + (t_m^3 + 4t_m)\hat{u}_m^5 - t_m \right)^2 + \left(t_m \hat{v}_m'' + 4\hat{v}_m' + t_m \hat{u}_m \hat{v}_m - (4t_m^3 + 5t_m)\hat{u}_m^3 - t_m \right)^2 \right) + \frac{1}{4} \left((\hat{u}_0 - 1)^2 + (\hat{v}_0 - 1)^2 + (\hat{u}_0')^2 + (\hat{v}_0')^2 \right) \quad (17)$$

Optimization of all three examples of EFS is supported with the hybrid of GA-SQP for 100 multiple runs to achieve the modifiable networks parameters. Set of weights is also plotted in Fig. 3 for $u(t)$ and $v(t)$. These weights are used to find the approximate solution for all three examples. The mathematical form is given as:

$$\hat{u}_{p-1} = \frac{0.4388}{1 + e^{-(5.2407t - 2.4439)}} + \frac{6.4835}{1 + e^{-(1.8582t - 2.4439)}} + \dots + \frac{1.3676}{1 + e^{-(1.9377t - 0.7522)}}, \quad (18)$$

$$\hat{u}_{p-2} = \frac{20}{1 + e^{-(4.8372t - 8.2022)}} + \frac{-0.6866}{1 + e^{-(0.4691t + 13.4365)}} + \dots + \frac{7.4195}{1 + e^{-(7.5298t + 11.4087)}}, \quad (19)$$

$$\hat{u}_{p-3} = \frac{-0.4823}{1 + e^{-(0.2095t + 0.7312)}} + \frac{-0.2412}{1 + e^{-(2.099t + 1.2441)}} + \dots + \frac{1.8088}{1 + e^{-(2.9497t + 1.1619)}}, \quad (20)$$

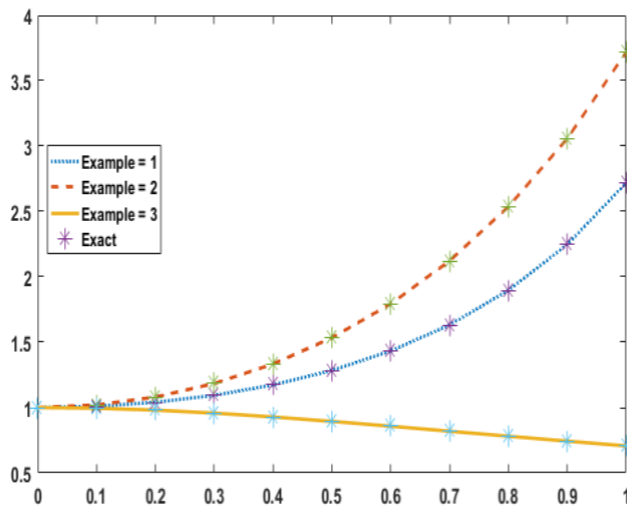
$$\hat{v}_{p-1} = \frac{-0.1392}{1 + e^{-(1.0314t + 1.3248)}} + \frac{-0.9027}{1 + e^{-(2.2836t - 0.5579)}} + \dots + \frac{0.1624}{1 + e^{-(0.8473t + 1.5818)}}, \quad (21)$$

$$\hat{v}_{p-2} = \frac{4.3832}{1 + e^{-(14.5169t + 9.1492)}} + \frac{-9.1174}{1 + e^{-(10.7660t - 14.6074)}} + \dots + \frac{-8.3274}{1 + e^{-(2.9999t - 11.4678)}}, \quad (22)$$

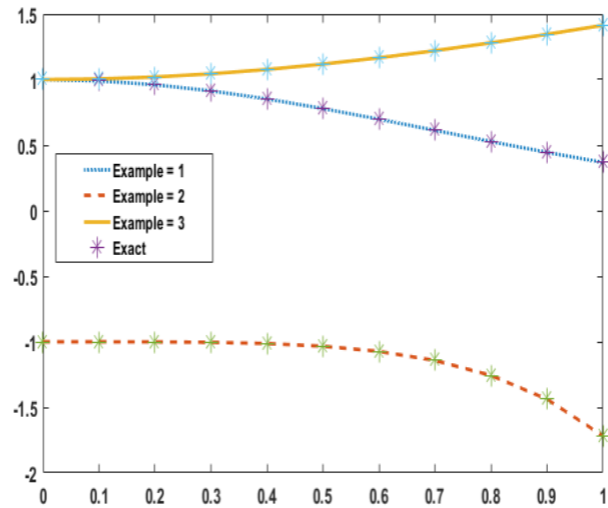
$$\hat{v}_{p-3} = \frac{3.8293}{1 + e^{-(0.9012t - 4.4533)}} + \frac{2.5218}{1 + e^{-(0.3953t - 14.1205)}} + \dots + \frac{2.4976}{1 + e^{-(0.8348t - 1.6292)}}. \quad (23)$$

The approximate values $\hat{u}(t)$ and $\hat{v}(t)$ by using equations (18-23) are plotted in Fig. 2. The overlapping of the proposed and exact solution for all three examples is also presented in Fig. 2. Absolute error (AE) is presented in Fig. 3 to assess the similarities of the results for both parameters of all three examples. The AE value for $\hat{u}(t)$ lie around 10^{-5} to 10^{-6} , 10^{-5} to 10^{-7} and 10^{-6} to 10^{-7} , while $\hat{v}(t)$ lie around 10^{-6} to 10^{-8} , 10^{-5} to 10^{-7} and 10^{-6} to 10^{-7} for example (1-3). The scale of fitness, MAD, RMSE, and EVAF based on performance measures for $u(t)$ and $v(t)$ are also plotted in Fig. 3. The optimal values are observed for all the performance indices that establish the value of the proposed scheme. Fig. 4 depicts the fitness and histogram plots for all three examples. It is clear in understanding that almost 75% of independent executions attained best fitness values for the examples 1, 2 and 3. The outcomes for MAD, RMSE and EVAF are drawn in Figs (5-7) along with the histogram plots. The results indicate that about 80% runs attain precise standards of MAD, RMSE and EVAF.

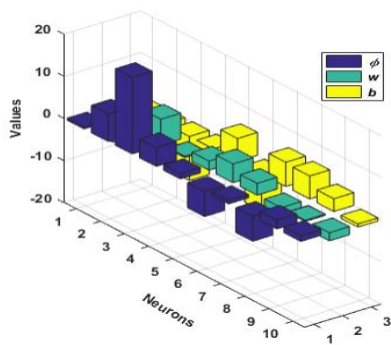
For the precision of the proposed scheme, statistical analysis is established on the basis of minimum (Min), mean (Mean) and standard deviation (SD). The results of these operators for examples (1-3) are tabulated in Tables 2 (a-b) for $\hat{u}(t)$ and $\hat{v}(t)$. The Min, Mean and SD values for each problem lie around 10^{-6} to 10^{-10} , 10^{-02} to 10^{-06} and 10^{-01} to 10^{-05} for both of the functions $\hat{u}(t)$ and $\hat{v}(t)$. The accuracy degraded for Mean values and SD values due to the effect of only one bad run can affect the mean values significantly. Table 3 presents the global performance operators GMAD, GRMSE and GVAF for the index $\hat{u}(t)$ and $\hat{v}(t)$ for 100 independent execution. It is observed that these operator values lie in good ranges. To find the proposed scheme performance, convergence analysis is made for various performance metrics and outcomes are presented in Table 4 for both $\hat{u}(t)$ and $\hat{v}(t)$. The results are clear that a large number of independent runs attain the level of accuracy. While for comparatively harder standards, the number of runs decreased extensively, but a proficient number of runs still there to achieve that level of accuracy. In order to find the algorithm computational cost, implementation/execution time values, number of cycle/iteration and counts of function for the networks are listed in Table 5 for the EFS.



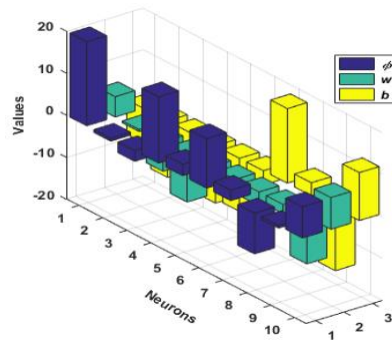
(a): Results of $\hat{u}(t)$ for Example (1-3)



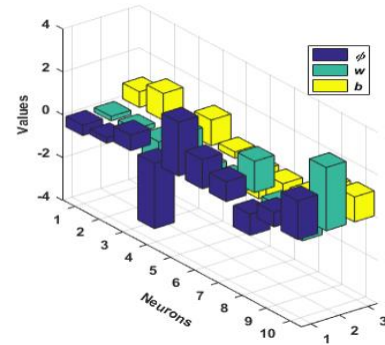
(b): Results of $\hat{v}(t)$ for Example (1-3)



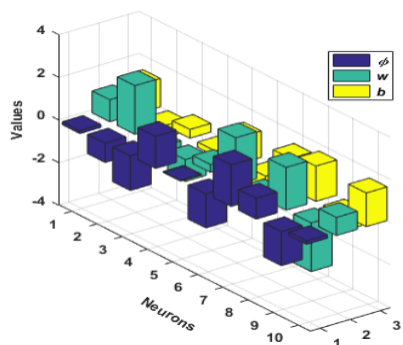
(c): $\hat{u}(t)$ weights for Example 1



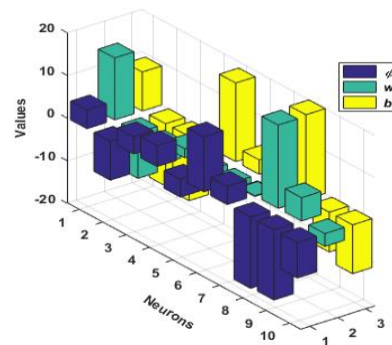
(d): $\hat{u}(t)$ weights for Example 2



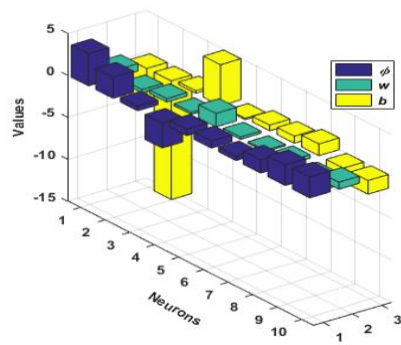
(e): $\hat{u}(t)$ weights for Example 3



(f): $\hat{v}(t)$ weights for Example 1

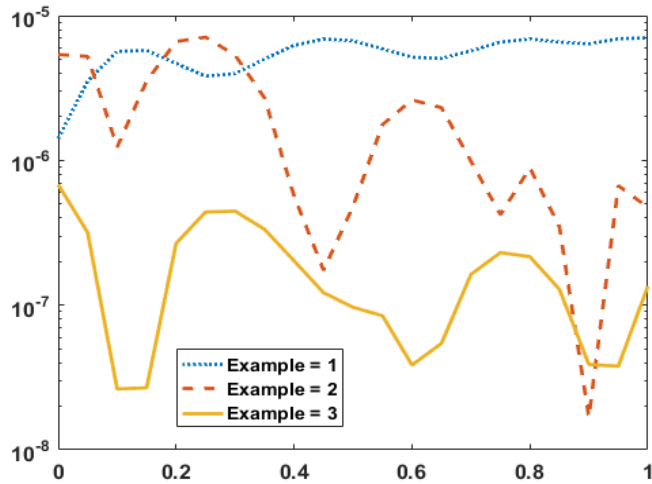


(g): $\hat{v}(t)$ weights for Example 2

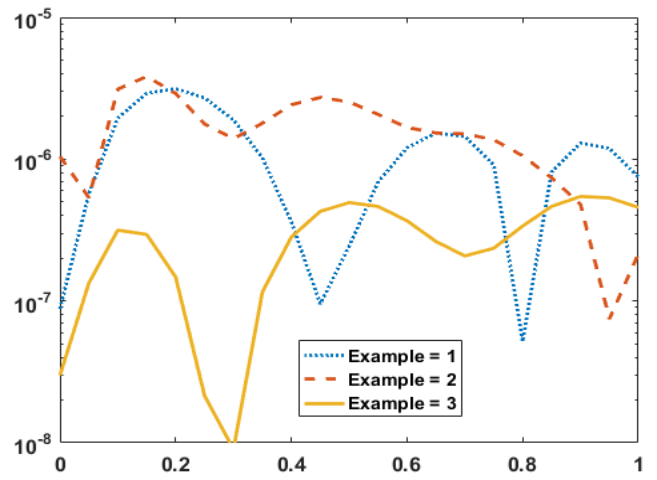


(h): $\hat{v}(t)$ weights for Example 3

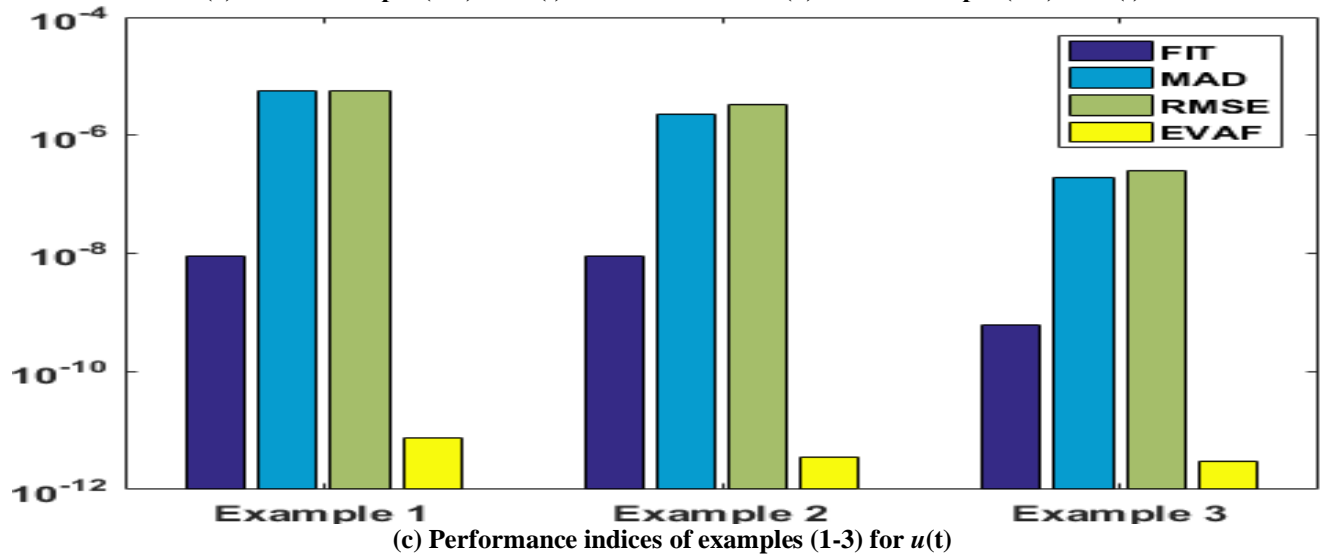
Fig 2: Set of weights and comparison of outcomes for Example (1-3)



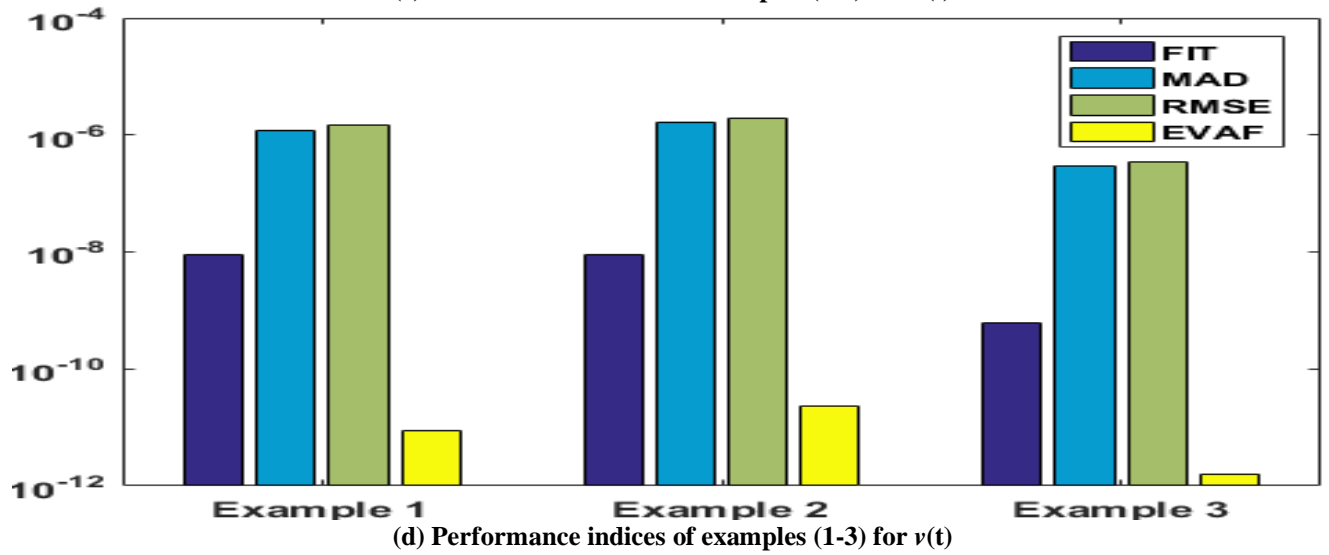
(a) AE of Example (1-3) for $u(t)$



(b) AE of Example (1-3) for $v(t)$

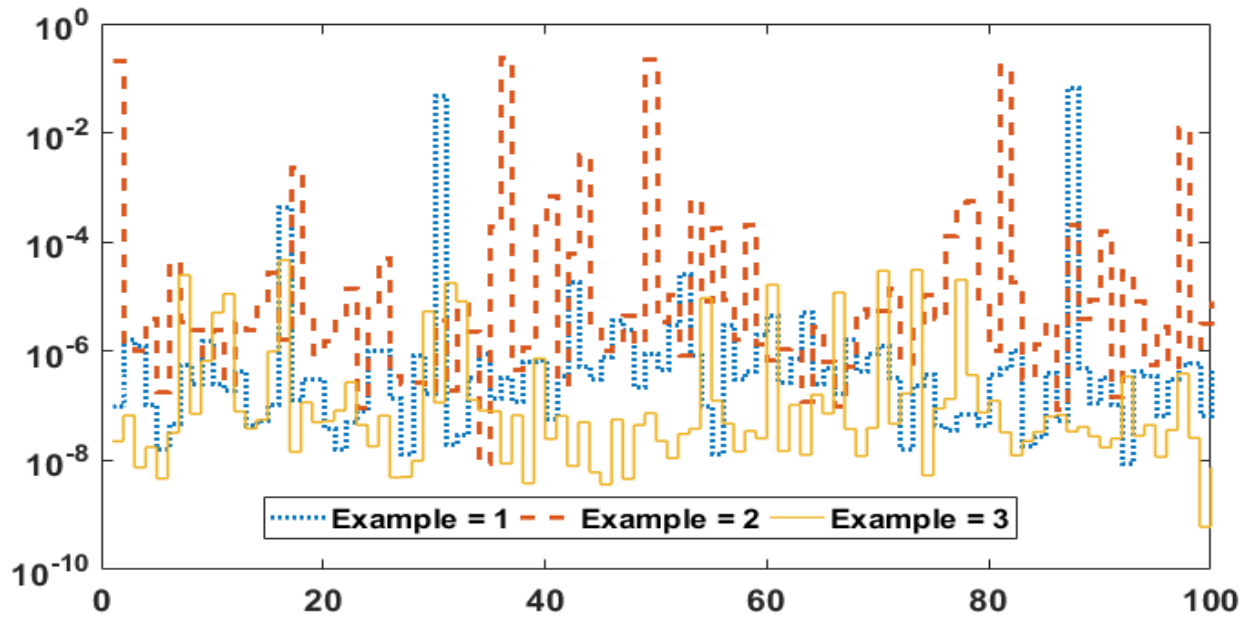


(c) Performance indices of examples (1-3) for $u(t)$



(d) Performance indices of examples (1-3) for $v(t)$

Fig 3: Absolute Error and Performance measures for Example (1-3)



Fitness value in convergence analysis for Examples (1-3)

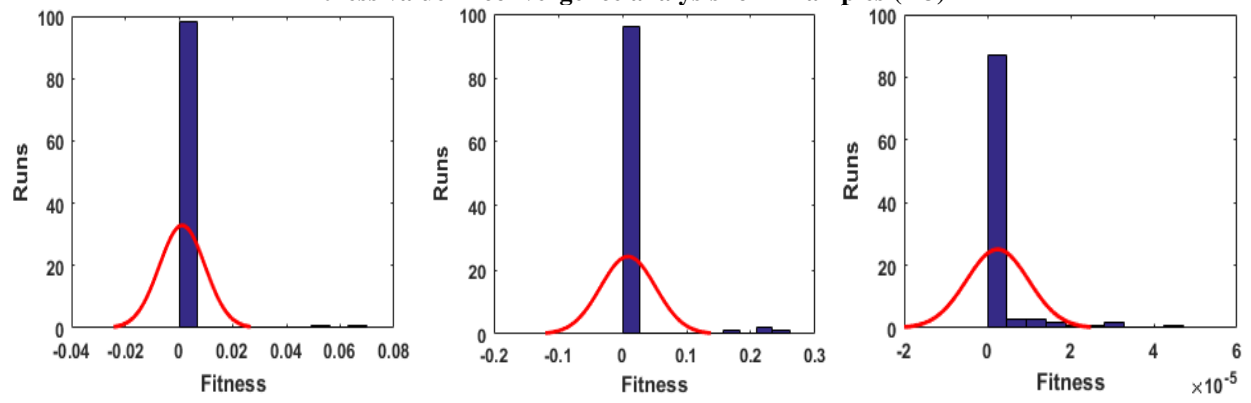
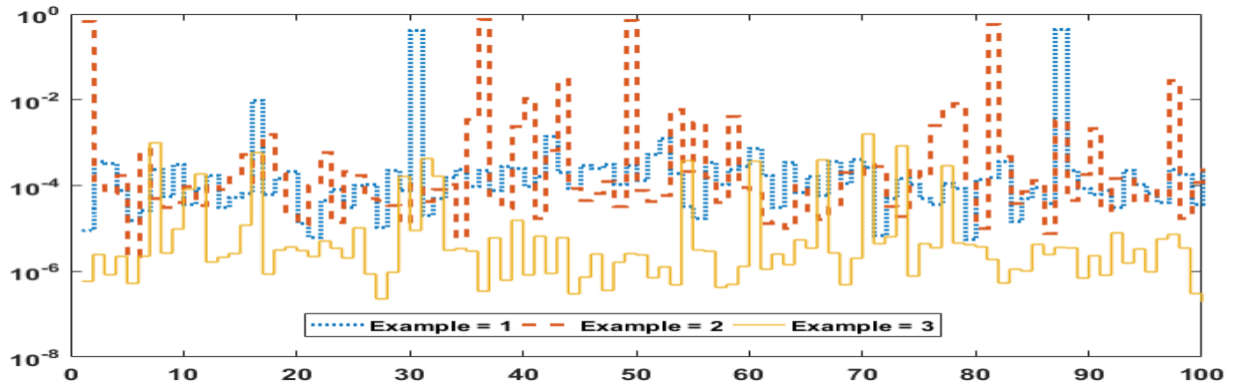
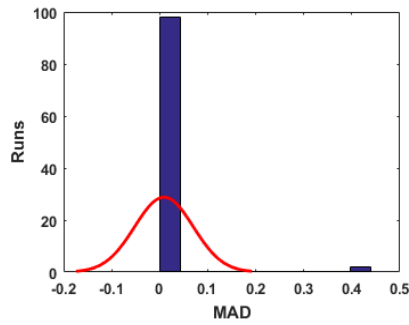


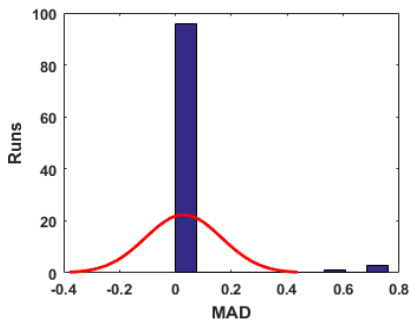
Fig 4: Fitness value and histogram of GA-SQP for Example (1-3)



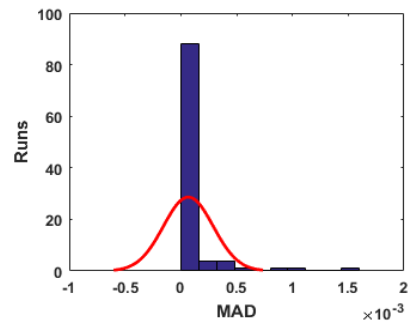
MAD value in convergence analysis for $u(t)$



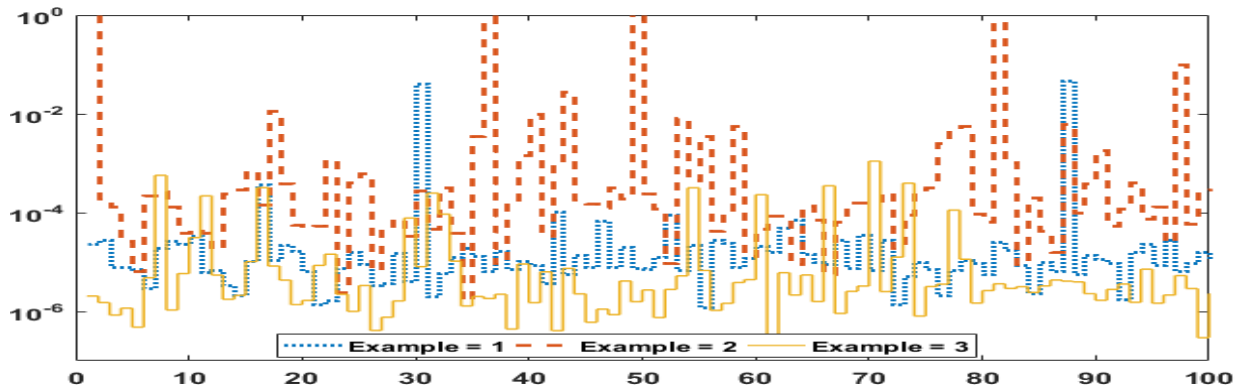
(a) Histogram for Example 1



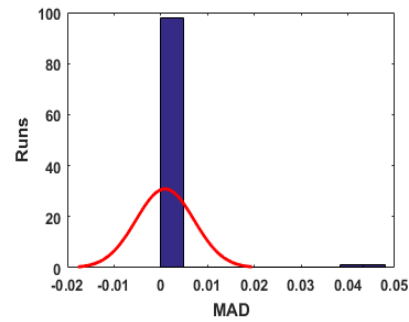
(b) Histogram for Example 2



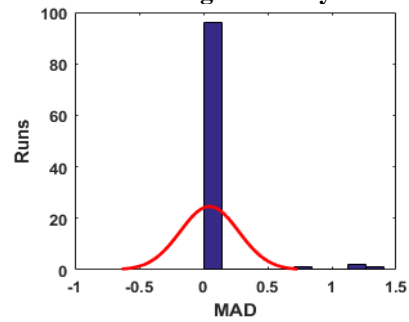
(c) Histogram for Example 3



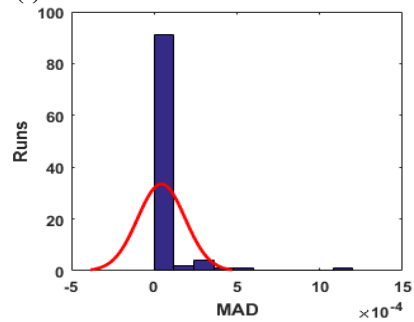
MAD value in convergence analysis for $v(t)$



(d) Histogram for Example 1



(e) Histogram for Example 2



(f) Histogram for Example 3

Fig 5: MAD value and histogram of GA-SQP for Example (1-3)

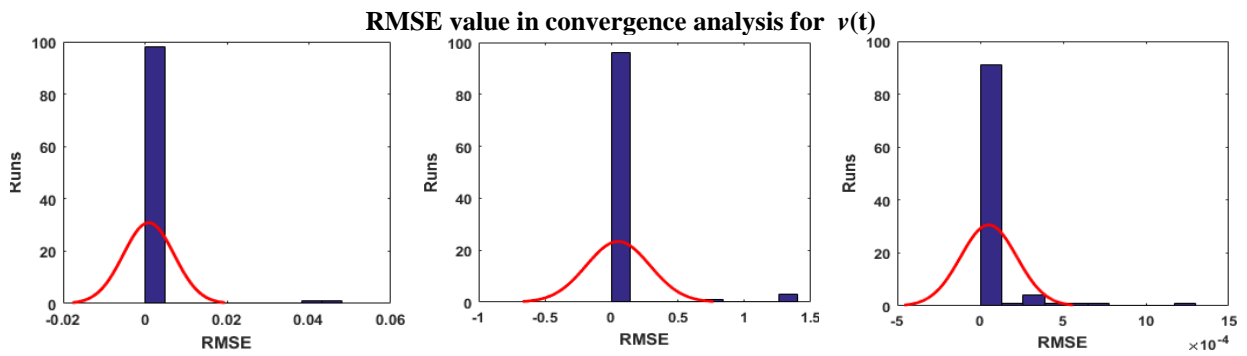
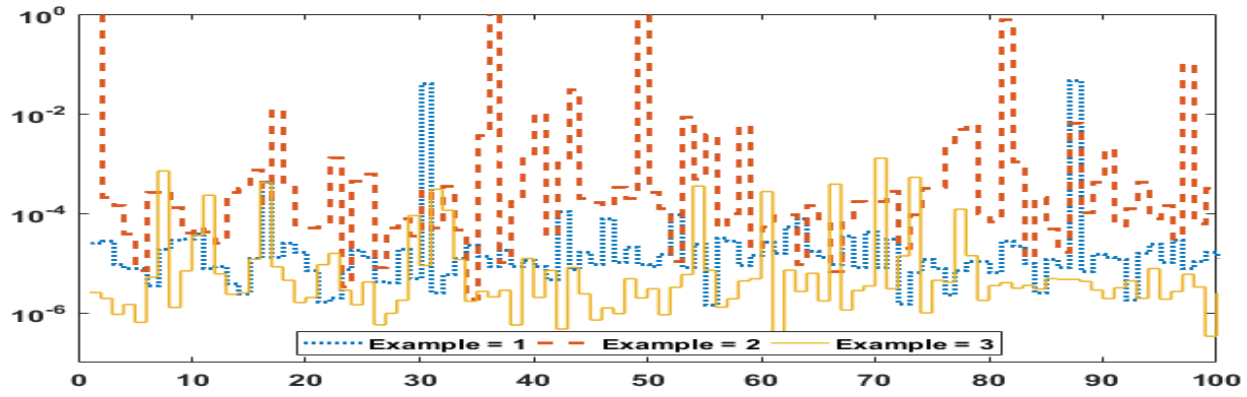
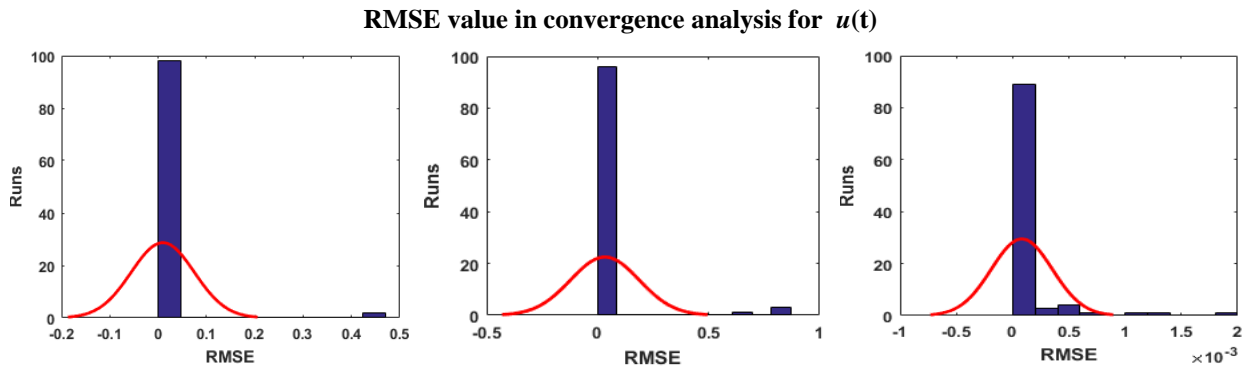
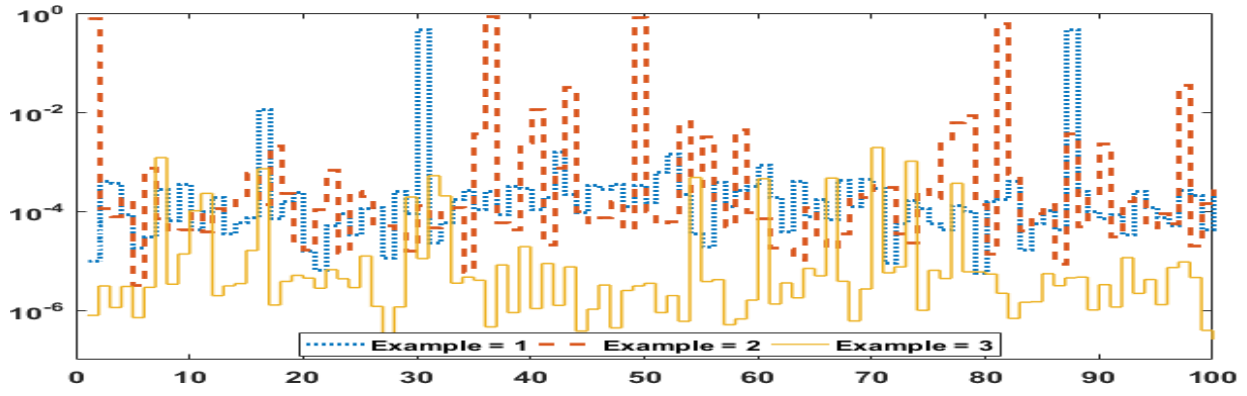
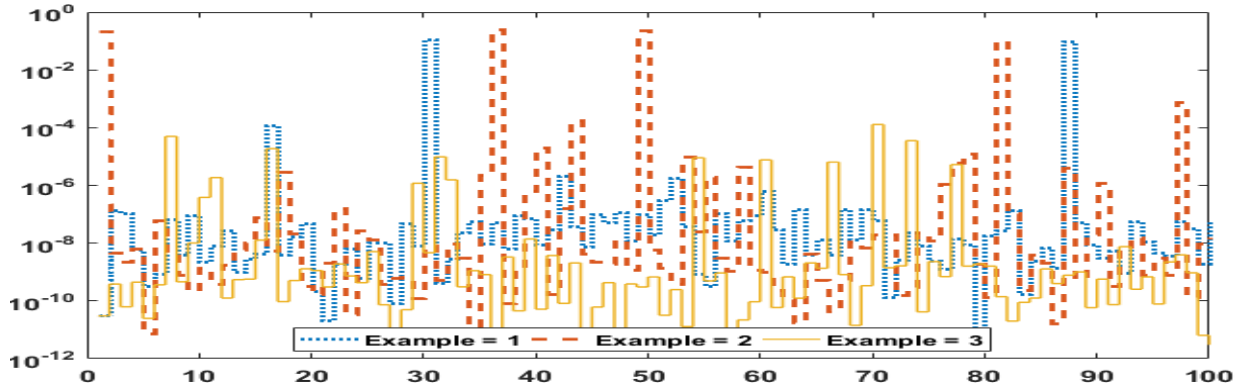
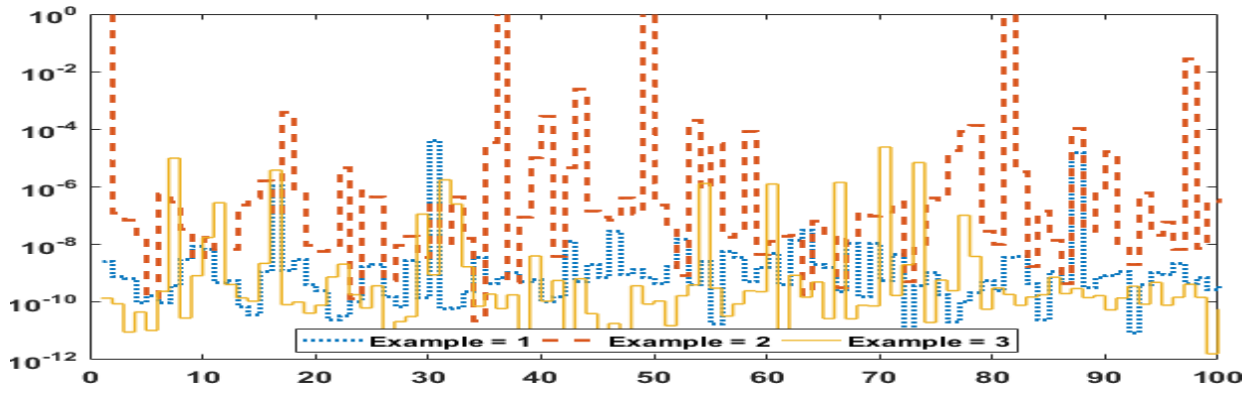
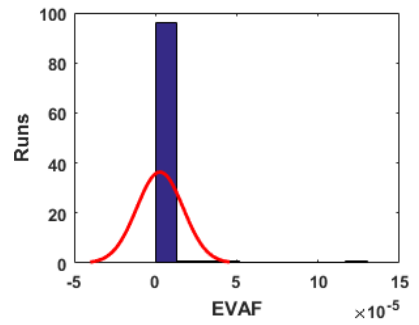
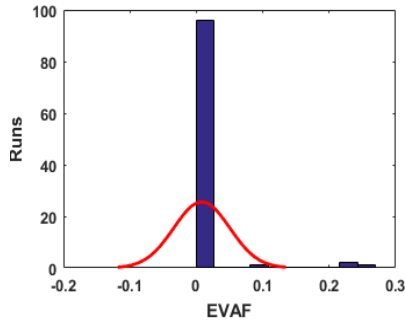
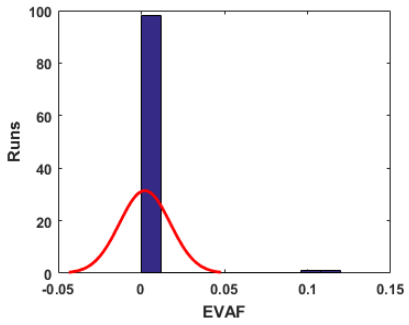


Fig 6: RMSE value and histogram of GA-SQP for Example (1-3)



EVAF value in convergence analysis for $u(t)$



EVAF value in convergence analysis for $v(t)$

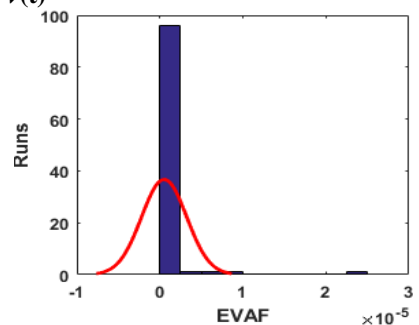
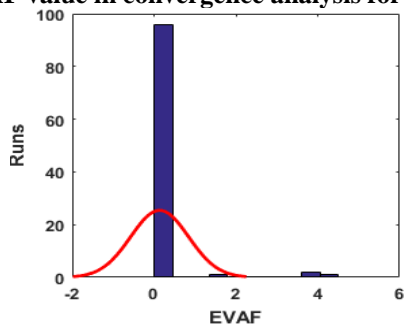
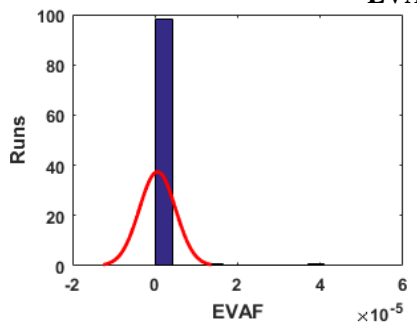


Fig 7: EVAF value and histogram of GA-SQP for Example (1-3)

Table 2 (a): Statistics outcomes of $\hat{u}(t)$ for all Examples

t	Example 1			Example 2			Example 3		
	Min	Mean	SD	Min	Mean	SD	Min	Mean	SD
0	2.13E-08	5.21E-03	3.78E-02	2.70E-08	1.59E-02	6.07E-02	2.91E-08	1.23E-04	4.59E-04
0.1	7.01E-07	5.43E-03	3.76E-02	1.52E-06	1.41E-02	6.27E-02	2.76E-08	1.52E-04	4.15E-04
0.2	1.52E-08	5.84E-03	4.04E-02	8.69E-07	1.52E-02	7.32E-02	7.56E-08	1.61E-04	3.72E-04
0.3	2.94E-06	6.36E-03	4.33E-02	2.71E-06	1.75E-02	8.40E-02	6.84E-09	1.80E-04	3.53E-04
0.4	1.85E-06	7.05E-03	4.72E-02	3.17E-07	2.04E-02	9.62E-02	4.03E-09	9.25E-05	3.14E-04
0.5	3.73E-06	7.84E-03	5.31E-02	4.38E-07	2.33E-02	1.91E-01	1.59E-08	7.15E-05	2.47E-04
0.6	5.20E-06	8.93E-03	6.14E-02	2.46E-06	2.82E-02	1.73E-01	1.11E-08	5.71E-05	1.75E-04
0.7	5.71E-06	1.07E-02	7.05E-02	9.59E-07	3.43E-02	1.56E-01	1.94E-08	2.78E-05	9.83E-05
0.8	6.94E-06	1.28E-02	8.16E-02	8.69E-07	4.14E-02	2.60E-01	7.95E-10	1.43E-05	4.82E-05
0.9	6.42E-06	1.49E-02	9.67E-02	1.77E-08	5.25E-02	2.25E-01	2.06E-09	5.37E-06	1.71E-05
1	7.07E-06	1.72E-02	1.18E-01	4.37E-07	6.57E-02	3.41E-01	1.37E-09	3.09E-06	1.30E-05

Table 2 (b): Statistics outcomes of $\hat{v}(t)$ for all Examples

t	Example 1			Example 2			Example 3		
	Min	Mean	SD	Min	Mean	SD	Min	Mean	SD
0	9.43E-11	8.76E-04	6.12E-03	2.05E-07	3.12E-02	1.53E-01	1.16E-10	1.56E-05	5.68E-05
0.1	4.42E-07	8.97E-04	6.14E-03	2.82E-07	3.23E-02	1.66E-01	3.14E-07	2.60E-05	6.50E-05
0.2	6.35E-07	9.04E-04	6.25E-03	5.47E-07	3.34E-02	1.67E-01	1.13E-09	2.72E-05	6.48E-05
0.3	2.47E-07	9.50E-04	6.26E-03	9.31E-07	3.16E-02	1.78E-01	9.02E-09	2.84E-05	8.31E-05
0.4	8.61E-08	9.60E-04	6.27E-03	3.24E-07	3.38E-02	1.86E-01	2.32E-08	2.97E-05	9.28E-05
0.5	2.74E-07	9.08E-04	6.22E-03	8.64E-07	4.42E-02	2.05E-01	4.94E-08	3.97E-05	1.13E-04
0.6	2.56E-07	9.05E-04	6.28E-03	1.79E-06	4.56E-02	2.24E-01	4.35E-08	5.32E-05	1.48E-04
0.7	1.36E-07	8.99E-04	6.29E-03	1.39E-08	5.82E-02	2.53E-01	4.36E-09	6.24E-05	2.62E-04
0.8	5.72E-08	9.01E-04	6.28E-03	1.14E-06	6.70E-02	2.92E-01	1.58E-08	7.10E-05	2.75E-04
0.9	1.91E-07	8.80E-04	6.27E-03	4.83E-07	7.61E-02	3.41E-01	3.39E-08	7.43E-05	2.86E-04
1	1.08E-07	9.10E-04	6.26E-03	2.12E-07	8.54E-02	4.06E-01	8.99E-09	7.54E-05	2.87E-04

Table 3: Global performance results of $\hat{u}(t)$ and $\hat{v}(t)$ for all Examples

Index	Example	GFIT		GMAD		GRMSE		GVAF	
		Magnitude	SD	Magnitude	SD	Magnitude	SD	Magnitude	SD
$\hat{u}(t)$	1	1.19E-03	8.49E-03	8.94E-03	6.14E-02	9.26E-03	6.57E-02	2.16E-03	1.52E-02
	2	8.88E-03	4.29E-02	2.87E-02	1.36E-01	3.25E-02	1.54E-01	8.20E-03	4.22E-02
	3	2.46E-06	7.48E-06	6.73E-05	2.23E-04	8.22E-05	2.71E-04	2.76E-06	1.43E-05
$\hat{v}(t)$	1	1.19E-03	8.49E-03	8.97E-04	6.20E-03	9.00E-05	6.20E-03	5.79E-07	4.37E-06
	2	8.87E-03	4.28E-02	4.74E-02	2.27E-01	4.99E-02	2.39E-01	1.36E-01	7.06E-01
	3	2.46E-06	7.78E-06	4.39E-05	1.48E-04	5.27E-05	1.68E-04	5.16E-07	2.72E-06

Table 4: Convergence analysis for problems (1-3)

Index	Ex	FIT \leq			MAD \leq			RMSE \leq			ENSE \leq		
		10-04	10-05	10-06	10-03	10-04	10-05	10-03	10-04	10-05	10-07	10-08	10-09
$\hat{u}(t)$	1	98	97	94	97	93	22	97	93	20	94	69	34
	2	89	80	60	90	78	33	90	77	30	82	77	54
	3	100	100	87	100	96	87	100	95	87	88	87	82
$\hat{v}(t)$	1	98	97	94	98	98	93	98	98	92	97	97	86
	2	89	80	60	88	77	27	87	77	21	72	45	16
	3	100	100	87	100	98	88	100	97	88	92	88	87

Table 5: Complexity analysis for problems (1-3)

Example	Implementation Time		Iterations		Function Values	
	Mean	SD	Mean	SD	Mean	SD
1	539.2775994	4612.871109	847.29	60.46357865	116627.45	17373.14954
2	97.91541211	243.6168986	856.18	38.09912112	110510.22	9469.53933
3	199.2706581	1181.289639	842.87	75.80126262	119546.38	19841.77236

4. Conclusion

The motivation behind this study is to solve singular system of Emden-Fowler model using ANNs optimized with GA, SQP and the hybrid of GA-SQP. Some key findings of the present study are summarized as:

- ANN applied effectively for solving the singular system of Emden-Fowler equation. By using the ANNs, the achieved outcomes using the proposed mythology are very accurate and reliable.
- To analyze the accuracy and convergence of the present method, statistical analysis is made for 100 independent runs to solve the model equation.
- The best AE values lie up to 10-05 to 10-09. However, the worst outcomes of AE lie up to 10-01 to 10-05.
- The statistical operators MAD, RMSE and VAF and their global forms are presented effectively with good agreements.

References

- [1] Luo, T., Xin, Z. and Zeng, H., 2016. Nonlinear asymptotic stability of the Lane-Emden solutions for the viscous gaseous star problem with degenerate density dependent viscosities. *Communications in Mathematical Physics*, 347(3), pp. 657-702.
- [2] Bhrawy, A. H., Alofi, A. S. and Van Gorder, R. A., 2014, May. An efficient collocation method for a class of boundary value problems arising in mathematical physics and geometry. In *Abstract and Applied Analysis* (Vol. 2014). Hindawi Publishing Corporation.
- [3] Rach, R., Duan, J. S. and Wazwaz, A. M., 2014. Solving coupled Lane-Emden boundary value problems in catalytic diffusion reactions by the Adomian decomposition method. *Journal of Mathematical Chemistry*, 52(1), pp. 255-267.
- [4] Boubaker, K. and Van Gorder, R. A., 2012. Application of the BPES to Lane-Emden equations governing polytropic and isothermal gas spheres. *New Astronomy*, 17(6), pp. 565-569.
- [5] Khan, J. A., Raja, M. A. Z., Rashidi, M. M., Syam, M. I. and Wazwaz, A. M., 2015. Nature-inspired computing approach for solving non-linear singular Emden-Fowler problem arising in electromagnetic theory. *Connection Science*, 27(4), pp. 377-396.
- [6] Dehghan, M. and Shakeri, F., 2008. Solution of an integro-differential equation arising in oscillating magnetic fields using He's homotopy perturbation method. *Progress in Electromagnetics Research*, 78, pp. 361-376.
- [7] Ramos, J. I., 2003. Linearization methods in classical and quantum mechanics. *Computer Physics Communications*, 153(2), pp. 199-208.
- [8] Radulescu, V. and Repovš, D., 2012. Combined effects in nonlinear problems arising in the study of anisotropic continuous media. *Nonlinear Analysis: Theory, Methods and Applications*, 75(3), pp. 1524-1530.
- [9] Flockerzi, D. and Sundmacher, K., 2011. On coupled Lane-Emden equations arising in dusty fluid models. In *Journal of Physics: Conference Series* (Vol. 268, No. 1, p. 012006). IOP Publishing.
- [10] Ghergu, M. and Radulescu, V., 2007. On a class of singular Gierer-Meinhardt systems arising in morphogenesis. *Comptes Rendus Mathématique*, 344(3), pp. 163-168.
- [11] Bender, C. M., Milton, K. A., Pinsky, S. S. and Simmons Jr, L. M., 1989. A new perturbative approach to nonlinear problems. *Journal of Mathematical Physics*, 30(7), pp. 1447-1455.
- [12] Shawagfeh, N. T., 1993. Non perturbative approximate solution for Lane-Emden equation. *Journal of Mathematical Physics*, 34(9), pp. 4364-4369.
- [13] Liao, S., 2003. A new analytic algorithm of Lane-Emden type equations. *Applied Mathematics and Computation*, 142(1), pp. 1-16.
- [14] Nouh, M.I., 2004. Accelerated power series solution of polytropic and isothermal gas spheres. *New Astronomy*, 9(6), pp. 467-473.
- [15] Mandelzweig, V.B. and Tabakin, F., 2001. Quasilinearization approach to nonlinear problems in physics with application to nonlinear ODEs. *Computer Physics Communications*, 141(2), pp. 268-281.
- [16] Wazwaz A-M (2011) The variational iteration method for solving systems of equations of Emden-Fowler type. *Int J Comput Math* 88:3406-3415

- [17] Muatjetjeja B, Khalique CM (2010) Lagrangian approach to a generalized coupled Lane–Emden system: symmetries and first integrals. *Commun Nonlinear Sci Numer Simul* 15:1166–1171
- [18] Burke, E. K., Gendreau, M., Hyde, M., Kendall, G., Ochoa, G., Ozcan, E. and Qu, R., 2013. Hyper-heuristics: A survey of the state of the art. *Journal of the Operational Research Society*, 64(12), pp. 1695-1724.
- [19] Pappa, G. L., Ochoa, G., Hyde, M. R., Freitas, A. A., Woodward, J. and Swan, J., 2014. Contrasting meta-learning and hyper-heuristic research: the role of evolutionary algorithms. *Genetic Programming and Evolvable Machines*, 15(1), pp. 3-35.
- [20] Raja, M. A. Z., Zameer, A., Khan, A.U. and Wazwaz, A.M., 2016. A new numerical approach to solve Thomas–Fermi model of an atom using bio-inspired heuristics integrated with sequential quadratic programming. *Springer Plus*, 5(1), p. 1400.
- [21] Soize, C., 2012, September. *Stochastic models of uncertainties in computational mechanics*. Reston: American Society of Civil Engineers.
- [22] Sabir, Z., Wahab, H.A., Umar, M. and Erdoğan, F., 2019. Stochastic numerical approach for solving second order nonlinear singular functional differential equation. *Applied Mathematics and Computation*, 363, p.124605.
- [23] Zhang, Z., El-Moselhy, T. A., Elfadel, I. M. and Daniel, L., 2013. Stochastic testing method for transistor-level uncertainty quantification based on generalized polynomial chaos. *IEEE Transactions on Computer-Aided Design of Integrated Circuits and Systems*, 32(10), pp. 1533-1545.
- [24] Raja, M. A. Z., Shah, F. H., Alaidarous, E. S. and Syam, M. I., 2017. Design of bio-inspired heuristic technique integrated with interior-point algorithm to analyze the dynamics of heartbeat model. *Applied Soft Computing*, 52, pp. 605-629.
- [25] He, W., Chen, Y. and Yin, Z., 2016. Adaptive neural network control of an uncertain robot with full-state constraints. *IEEE Transactions on Cybernetics*, 46(3), pp. 620-629.
- [26] Schaff, J. C., Gao, F., Li, Y., Novak, I. L. and Slepchenko, B. M., 2016. Numerical Approach to Spatial Deterministic-Stochastic Models Arising in Cell Biology. *PLoS computational biology*, 12(12), p. e1005236.
- [27] Pelletier, F., Masson, C. and Tahan, A., 2016. Wind turbine power curve modelling using artificial neural network. *Renewable Energy*, 89, pp. 207-214.
- [28] Manik, S., Saini, L. M. and Vadera, N., 2016, July. Counting and classification of white blood cell using Artificial Neural Network (ANN). In *Power Electronics, Intelligent Control and Energy Systems (ICPEICES)*, IEEE International Conference on (pp. 1-5). IEEE. algorithms. *Evolutionary computation*, 2(3), pp. 221-248.
- [29] Sridhar, R., M. Chandrasekaran, C. Srirama, and Tom Page. "Optimization of heterogeneous Bin packing using adaptive genetic algorithm." In *IOP Conference Series: Materials Science and Engineering*, vol. 183, no. 1, p. 012026. IOP Publishing, 2017.
- [30] Chang, F. S., 2016. Greedy-Search-based Multi-Objective Genetic Algorithm for Emergency Humanitarian Logistics Scheduling.
- [31] An, P. Q., Murphy, M. D., Breen, M.C. and Scully, T., 2016, August. One-day-ahead cost optimisation for a multi-energy source building using a genetic algorithm. In *Control (CONTROL)*, 2016 UKACC 11th International Conference on (pp. 1-6). IEEE.

- [32] Vaishnav, P., Choudhary, N. and Jain, K., 2017. Traveling Salesman Problem Using Genetic Algorithm: A Survey.
- [33] Das, S., Chaudhuri, S. and Das, A.K., 2017, February. Optimal Set of Overlapping Clusters Using Multi-objective Genetic Algorithm. In Proceedings of the 9th International Conference on Machine Learning and Computing (pp. 232-237). ACM.
- [34] Tuhus-Dubrow, D. and Krarti, M., 2010. Genetic-algorithm based approach to optimize building envelope design for residential buildings. *Building and environment*, 45(7), pp. 1574-1581.
- [35] Roberge, V., Tarbouchi, M. and Okou, F., 2016, May. New encoding based on the minimum spanning tree for distribution feeder reconfiguration using a genetic algorithm. In *Electrical and Information Technologies (ICEIT), 2016 International Conference on* (pp. 16-21). IEEE.
- [36] Lee, J. C., Lin, W. M., Liao, G. C. and Tsao, T. P., 2011. Quantum genetic algorithm for dynamic economic dispatch with valve-point effects and including wind power system. *International Journal of Electrical Power and Energy Systems*, 33(2), pp. 189-197.
- [37] Hoque, M. S., Mukit, M., Bikas, M. and Naser, A., 2012. An implementation of intrusion detection system using genetic algorithm. arXiv preprint arXiv: 1204.1336.
- [38] Tan, J. and Kerr, W. L., 2017. Determination of glass transitions in boiled candies by capacitance based thermal analysis (CTA) and genetic algorithm (GA). *Journal of Food Engineering*, 193, pp. 68-75.
- [39] Ball, M. G., Qela, B. and Wesolkowski, S., 2016. A Review of the Use of Computational Intelligence in the Design of Military Surveillance Networks. In *Recent Advances in Computational Intelligence in Defense and Security* (pp. 663-693). Springer International Publishing.
- [40] Pasandideh, S.H.R., Niaki, S.T.A. and Gharaei, A., 2015. Optimization of a multiproduct economic production quantity problem with stochastic constraints using sequential quadratic programming. *Knowledge-Based Systems*, 84, pp.98-107.
- [41] Subathra, M.S.P., Selvan, S.E., Victoire, T.A.A., Christinal, A.H. and Amato, U., 2015. A hybrid with cross-entropy method and sequential quadratic programming to solve economic load dispatch problem. *IEEE Systems Journal*, 9(3), pp.1031-1044.
- [42] Engelbrecht, J.J. and Engelbrecht, J.A., 2016, November. Optimal attitude and flight vector recovery for large transport aircraft using sequential quadratic programming. In *2016 Pattern Recognition Association of South Africa and Robotics and Mechatronics International Conference (PRASA-RobMech)* (pp. 1-7). IEEE.
- [43] Sun, Z., Tian, Y., Li, H. and Wang, J., 2016. A superlinear convergence feasible sequential quadratic programming algorithm for bipedal dynamic walking robot via discrete mechanics and optimal control. *Optimal Control Applications and Methods*, 37(6), pp.1139-1161.
- [44] Chaudhry, F.A., Amin, M., Iqbal, M., Khan, R.D. and Khan, J.A., 2018. A novel chaotic differential evolution hybridized with quadratic programming for short-term hydrothermal coordination. *Neural Computing and Applications*, 30(11), pp.3533-3544.